On calculation of stress-strain state of steel closed ropes in extension and twisting
Part 2. Influence of torsion on the stress-strain state of closed rope

***V. F. Danenko**, Cand. Eng., Associate Prof.*[1]*, e-mail: omd@vstu.ru;*
***L. M. Gurevich**, Dr. Eng., Associate Prof.*[1]

[1]*Volgograd State Technical University (Volgograd, Russia):*

Comparative analysis of the results of determination of stress-strain state in a closed lifting rope during extension and twisting was conducted via analytical calculation according to the linear static equations and computer-aided finite element modeling. Computer modeling allows to establish the features of variation of internal axial forces and torques in the layers that are laid with different directions. It makes possible to predict workability of a closed lifting rope during operation.
The most intensive redistribution of internal forces and torques in the internal and subsurface layers during rope turns under the effect of external torque was found out in comparison with extension. Decrease of the torque and axial force values to zero in the deposited external layer during its untwisting testifies about switching this layer off the operation and possibility of rope lamination in the case of external pressure absence. Internal compression of subsurface layer from the side of external rope layer, in its turn, decreases possibility of stability loss (opening) of this layer during its twisting.
Deviation from the common rule for variation features of relative elongation ε during joint extension and twisting was shown during modeling. So, external untwisting torque tries to extend the rope (increase of ε), while twisting torque tries to compress it (decrease of ε), what is connected with influence of gap values between the rope elements (wires and layers) on distribution of the contact stresses between them during twisting.
Key words: closed lifting rope, finite element modeling, stress-strain state, wire, rope layer, extension, twisting, force, torque, deformation.
DOI: 10.17580/cisisr.2022.01.08

Introduction

The approaches to determination of the stress-strain state (SSS) of ropes elements for providing their reliable and safe operation have been discussed in the work [1] and considered in the publications [2-7]. Essential role of computer-aided modeling on the base of the methods of finite element modeling (FEM) in rising SSS evaluation precision for ropes was noted; it used different software products [7-11]. It was mentioned that limited number of works in this area for closed ropes were presented.

Practically closed lifting rope often operates in the conditions of joint extension and torsion [12-15]. The generalized static equations during analytical rope SSS determination in the conditions of joint extension and torsion were presented in the work [1] as it had been suggested by M. F. Glushko [3]:

$$P = A \cdot \varepsilon + C \cdot \theta$$
$$M = C \cdot \varepsilon + B \cdot \theta \qquad (1)$$

where P – axial force; M – torque; ε and θ – relative elongation and torsion deformations; A, B and C – generalized stiffness coefficients.

Solutions of the equations (1) relating to deformations ε and θ can be displayed as [3]

$$\varepsilon = \frac{B}{\Delta} \cdot P - \frac{C}{\Delta} \cdot M; \qquad (2)$$

$$\theta = -\frac{C}{\Delta} \cdot P + \frac{A}{\Delta} \cdot M \qquad (3)$$

where $\Delta = A \cdot B - C^2$.

Torsion initiates variation of stress state in rope elements, what has the effect on its operating reliability [8, 16, 17]. Based on the [3] data, singular torque causes larger stresses in rope in comparison with singular axial force. Influence of torsion on stress state in rope elements can be evaluated via analysis of relationships between normal stresses σ_p and axial extension in cross section of spiral laid wire [3]

$$\sigma_p = E\varepsilon_s = E(\varepsilon \cos^2\alpha + \theta r \sin\alpha \cos\alpha) = \sigma_p^* + \sigma_p^{**}, \qquad (4)$$

where E – elasticity modulus of wires materials; ε_s – relative elongation of spiral laid wire; r and α – wire radius and laying angle, respectively.

For the equation (4), the relationship between normal stress components and extension $\sigma^*_p = E\varepsilon\cos^2\alpha$ as well as between normal stress components and torsion $\sigma_p^{**} = E\theta r \sin\alpha \cos\alpha$ can be presented as

$$\frac{\sigma_p^{**}}{\sigma_p^*} = a_1 \cdot r \cdot \mathrm{tg}\alpha > 1 \qquad (5)$$

The analysis displays that the relationship (5) in connection with the standard values for spiral ropes

$a_1 = \theta/\varepsilon = 2.0\text{-}3.7$ mm^{-1} [3], for laying angle $\alpha = 15\text{-}20^{\circ}$ and for rope diameter from 20 to 50 mm is executed in accordance with the GOST 10506-76. It confirms exceeding of the normal stress component during rope torsion in comparison with extension ($\sigma_p^{**} > \sigma_p^{*}$). Computer-aided modeling of SSS variation allows to predict the influence of gaps and contact stresses values between rope elements on saving the rope structural integrity during operation.

Examination of the stress-strain state of rope elements during axial extension and torsion was conducted via the finite elements method using licensed software package SIMULIA/Abaqus. The rope consists of core *1* with 1+7+7/7+14 construction from wires with round cross section, consequent layer *4* from the same wires, sub-surface layer 5 from alternating wires with round and H-shape cross sections and external layer *6* with wires having Z- shape cross sections [1] (**Fig. 1**). The core is laying in three layers around the central straight wire during one technological operation, based on the principle of linear touching (LT) of wires layers. Laying of the consequent rope layers was conducted via separate technological operations via the point touching (PT) principle, with alternating laying direction for laying of wires layers. Squares of rope layers cross section make: 45.44 mm² for the layer *4*, 72.64 mm² for the layer *5*, 104.05 mm² for the layer *6* [1, 8].

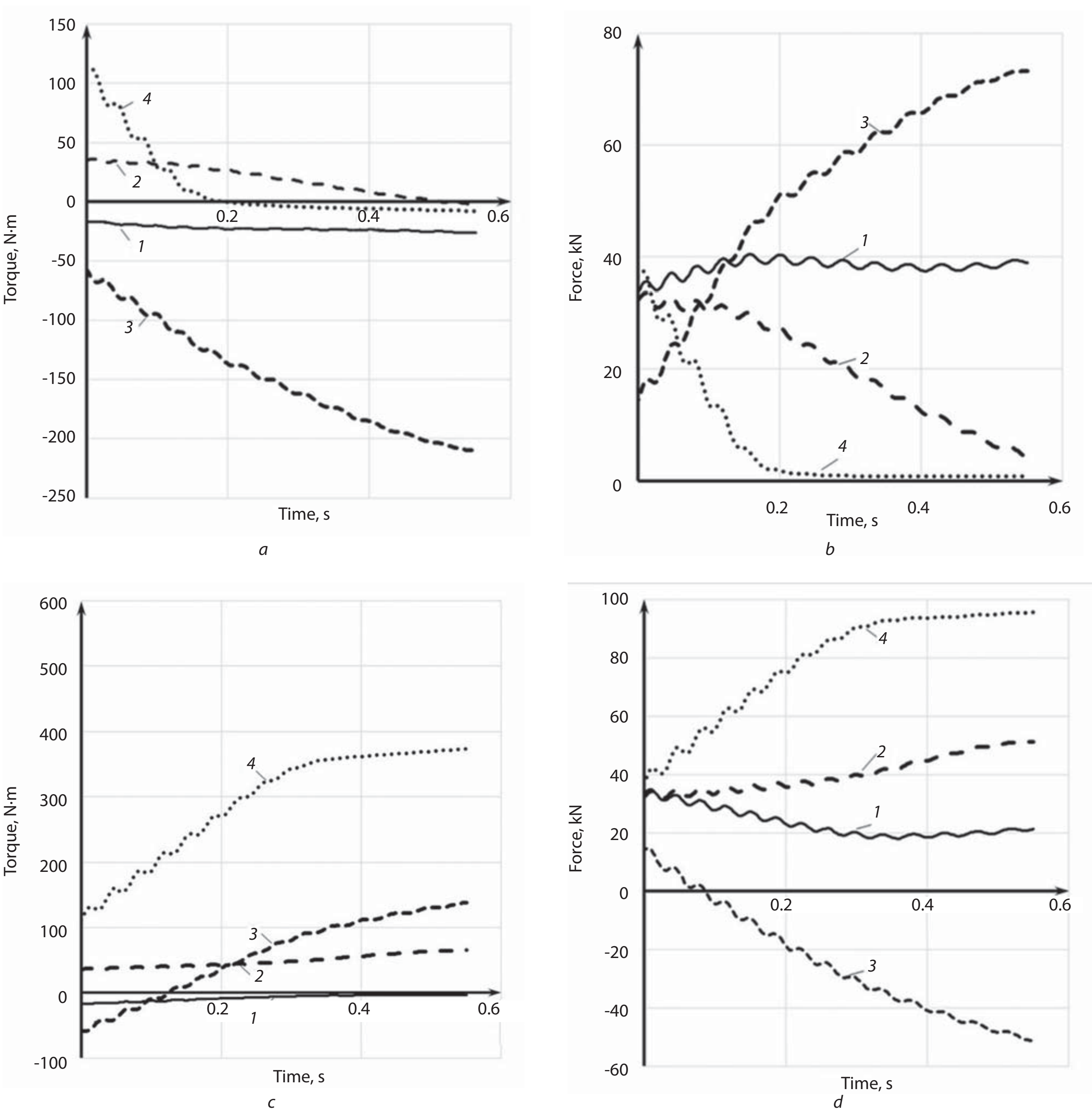

Fig. 1. Distribution of torques and axial forces in role layers at joint extension and torsion, for untwisting (a, b) and twisting (c, d) of the external layer for wires having Z-shape cross sections: 1 — core; 2 — layer 4; 3 - layer 5; 4 — layer 6.

The results of SSS modeling of rope elements during pure extension and pure torsion allowed to determine generalized stiffness coefficients *A*, *B* and *C*, as well as the values of linear ε and angular θ deformation at preset values of axial force *P* and torque *M* [1].

To provide modeling of transfer of longitudinal force and rotating motion (these conditions are typical for operation of the surface drive for a well pump [12, 13]), torsion of the rope sample by external torque *M* was conducted owing to turn of a movable stiff disc with velocity 36 °/s, with constant axial extension force *P*=120 kN and with possibility of disc axial displacement during turns (ε ≠ 0, θ ≠ 0). The torque which is directed to twisting of the external layer of a rope sample, was accepted to be positive. Wire edges of rope layers were strictly connected with the edge surface of a movable stiff disc in auxiliary equipment at the rear end, while at the front end they were connected with coaxially located stationary stiff disc, which was connected with the core and rings. The rings, in their turn, were connected with the rope layers [1]. All these connections provide equal edge displacements for all wires of rope fragment.

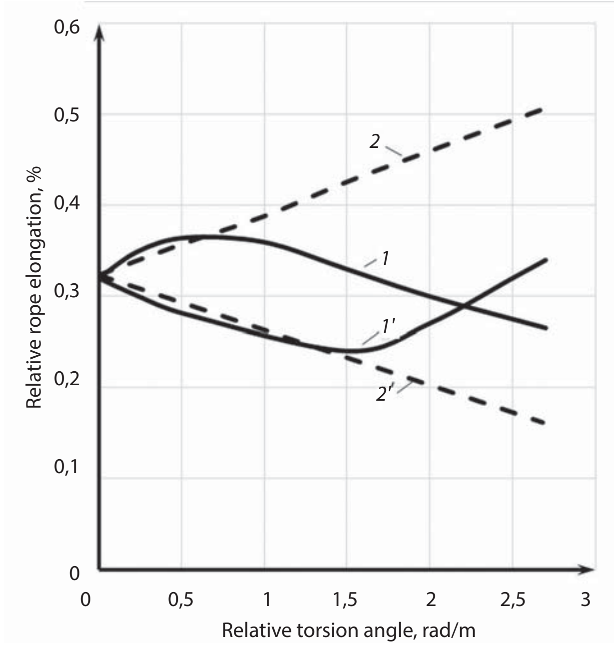

Fig. 2. Variation of relative elongation ε of the rope sample for joint extension and torsion: ——— - modeling; - - - - - analytical calculation; curves *1* and *2* – untwisting of the rope external layer, curves *1'* and *2'* – twisting of the rope external layer

Results and discussion

To examine the effect of torsion on rope SSS, the values distribution curves of internal torques and forces in each layer, which have been conducted were analyzed on the base of their modeling (Fig. 1).

Before the beginning of torsion (relative torsion angle θ = 0), the rope sample was under action of the axial extension force *P* ≈ 120 kN and the resulting torque M_t = 68.4 N·m [8], which was formed at axial extension. The rope layers are in the extended state. At the same time the torques M_t are positive in the layers *6* and *4* (they coincide with direction of layers laying) and negative in the layer *5* and in the core (opposite direction of layers laying) (Fig. 1, *a*, *c*).

When the rope is turning (the external layer of wires is subjected to untwisting or twisting turns) under the effect of external torque *M*, redistribution of the values of internal forces *P* and torques M_t in the rope layers occurs according the law of additional stresses. Based on the accepted conditions of fixing of layers with different laying directions on the wires edges of stiff discs and rings, the rope layers are striving to larger variation of dimensions at torsion in axial direction and transfer the extending forces to the layers, which are striving to smaller variation of their axial dimensions, and vice versa [8].

When the torque *M* is negative (untwisting of the rope external layer), laying directions of the layer *5* and core layers coincide with direction of external torque *M*, while wires of the layer *5* and core are compacted and are striving to reducing of axial length of the layers. Untwisting layers *4* and *6* prevent decreasing of the rope sample length. As a result, additional extending stresses appear in the layer *5* and in the core; it leads to increase of internal axial forces *P* (curves *3* and *1* on the Fig. 1, *b*). At the same time, compressing stresses appear in the layers *4* and *6*; they promote reducing of internal forces *P* in these layers (curves *2* and *4* on the Fig. 1, *b*). It is shown that axial force decreases practically to zero in the external layer, at the angle θ = 0,6-0,8 rad/m; deposited layer does not take up the axial load and is excluded from operation, what promotes rope lamination without any external pressure. Longitudinal stiffness of the rope is determined in this case only by other layers.

When the torque *M* is positive (twisting of the rope external layer), the picture is changing principally: the layers *4* and *6* are compacted under the effect of external torque *M* and are striving to length diminishing; as a result, the extending forces *P* in these layers elevate (curves *4* and *2* on the Fig. 1, *d*). The layer 5 and core layers are untwisting, the extending forces decrease (curves *3* and *1* on the Fig. 1, *d*). Axial forces in wires become compressing in the layer *5*, at the angle θ ≈ 0,4 rad/m; so the layer saves its stability only due to its subjecting to external compression from the side of external layer.

The results of modeling show that wires in the layers are compacted and are striving to decrease of the layer axial length, when laying direction coincides with layer torsion direction, and on the contrary, if directions of wire laying and torsion are opposite, the layers are laminated and are striving to increase the layer axial length. In the case of rope torsion under effect of external torque *M*, redistribution of internal forces *P* and torques M_t occurs with maximal intensity in the external and sub-surface layers (curves *3* and *4* on the Fig. 1).

The value of relative elongation ε = 0.323 %, which is initial for the stage of complex loading and was obtained in simulation of rope extension [1], can decrease or increase until end of this stage depending on the torque sign.

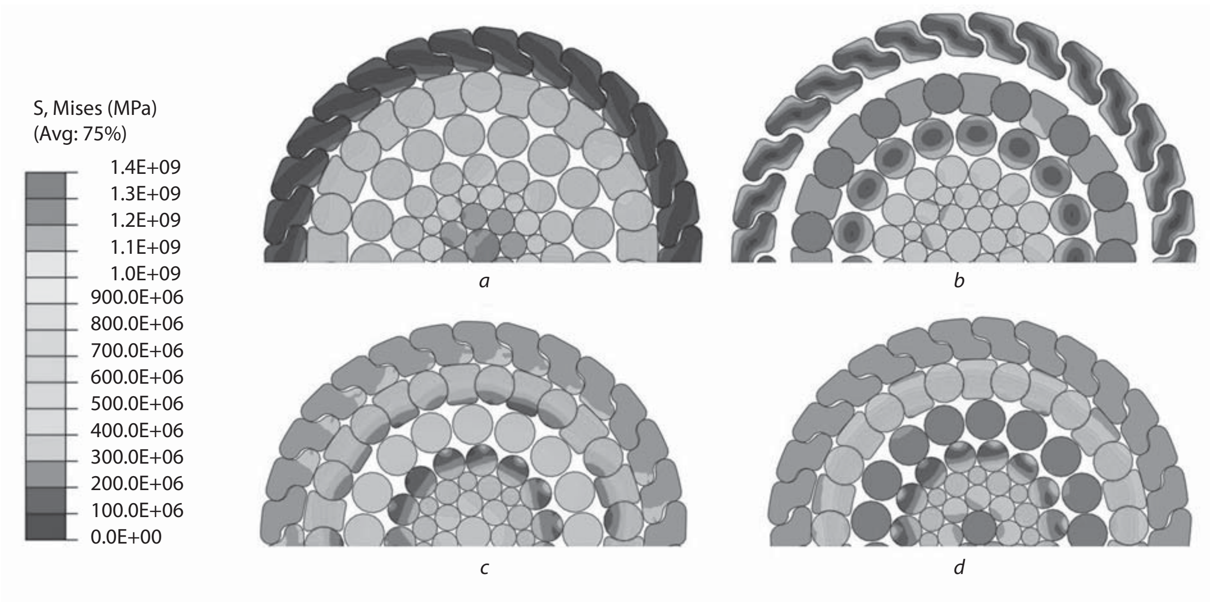

Fig. 3. Distribution of equivalent stresses in rope cross section during untwisting (θ = 0.8 rad/m (*a*) and θ = 2.68 rad/m (*b*), and during twisting θ = 1.5 rad/m (*c*) and θ = 2.68 rad/m (*d*)) of the external layer

In general case, for standard conditions, untwisting torque tries to extend rope (this is ε increase), while twisting torque tries to compress it (this is ε decrease). It is confirmed by the results of analytical calculation of relative elongation ε according to the equation (2), for rope untwisting (curve *2*) and for rope twisting (curve *2*') (**Fig. 2**). These results are obtained for preset values of force *P*, torque *M* and stiffness coefficients *A*, *B* and *C* got from the work [1]. The initial value of relative deformation ε is equal to 0.323 % for linear mode of its variation; it increases up to 0.506 % for rope sample untwisting and decreases to 0.162 % for its twisting.

However, the results of modeling testify about deviation of variation mode of relative elongation ε from the standard one (curves *1* and *1*' on the Fig. 2). It is connected with load redistribution between rope layers due to non-compliance of their transversal motions [18] and especially appears in rope torsion with opposite direction of layers laying. It is confirmed by Moses distribution of equivalent stresses σ_{eq} in cross sections of rope elements during torsion [8]. To provide coordinated narrowing of layers, it is necessary to lay them with definite circular gaps between the wires [3, 19, 20].

When the external layer is untwisting, standard increase of rope axial length up to the value ε = 0.375 % (curve 1 on the Fig. 2) at the initial period occurs due to untwisting of the layer *6*. The vales of the torque M_t and axial force *P* in the external layer decrease down to zero (curves *4* on the Fig. 1, *a* and *b*) for the relative torsion angle θ = 0.6-0.8 rad/m. Average values of stresses σ_{eq} in wires cross sections of external and sub-surface layers make $\sigma_{eq} \approx 100$ MPa and $\sigma_{eq} \approx 800$ MPa, respectively (**Fig. 3**, *a*). Intensive compaction of the layer *5* during twisting (curve *3* on the Fig. 1, *a*) causes decrease of the rope relative elongation in general down to ε = 0.263 % (curve *1* on the Fig. 2). Average stress values in wires cross sections of the layer 5 achieve $\sigma_{eq} \approx 1{,}100$ MPa for slight increase of stresses in wires cross section of the deposited (with gap forming) external layer (Fig 3, *b*).

When the external layer is twisting, the rope twisting layers *4* and 6 (Fig 3, *c* and *d*) are the most loaded. Standard decrease of rope relative deformation to the middle of stage to the value ε = 0.24 % (curve *1'* on the Fig. 2) occurs mainly due to compaction of wires in the layer *6*. The values of torque and axial force in the layer 6 achieve maximal values and become constant (curves *4* on the Fig. 1, *c* and *d*) for the relative torsion angle θ = 1.5 rad/m. Equivalent stresses in the wires cross sections of the external layer are distributed in uniform mode and constitute $\sigma_{eq} = 1{,}120$ MPa (Fig. 3, *c*). The untwisting layer *5*, providing contact pressure on the external layer owing to absence of radial gap between the rope layers *5* and *6* prevent compacting of this layer [19]. The contact stresses from the side of the layer 5 make $\sigma_{eq} \approx 700$ MPa (Fig. 3, *c*). Increase of the torque in the layer *5* (curve *3* on the Fig. 1, *c*), for the angle θ > 1.5 rad/m and for constant values of *M* in other layers, promotes uncoiling of wires in this layer and increase of relative deformation in the rope sample to the end of the twisting stage up to the value ε = 0.323 % (curve *1'* on the Fig. 2). As soon as the relative torsion angle increases, stresses in wires cross section of the layer 6 and on the contact between the layers *5* and *6* enlarge and make $\sigma_{eq} = 1{,}200$-$1{,}300$ MPa (Fig. 3, *d*) at θ = 2.68 rad/m. It exceeds the value of initial yield strength $\sigma_{so} = 1{,}120$ MPa for the wires with shaped section [8], which is preset for modeling, and leads to development of plastic deformation.

The resulting values of torques and forces in the conditions of joint extension and torsion, obtained via summarizing of the values of internal torques and forces in the each layer presented on the Fig. 1, are shown on the Fig. 4 (curves *1* and *1*'). The boundary torque values, with constant axial force $P \approx 120$ kN, make:

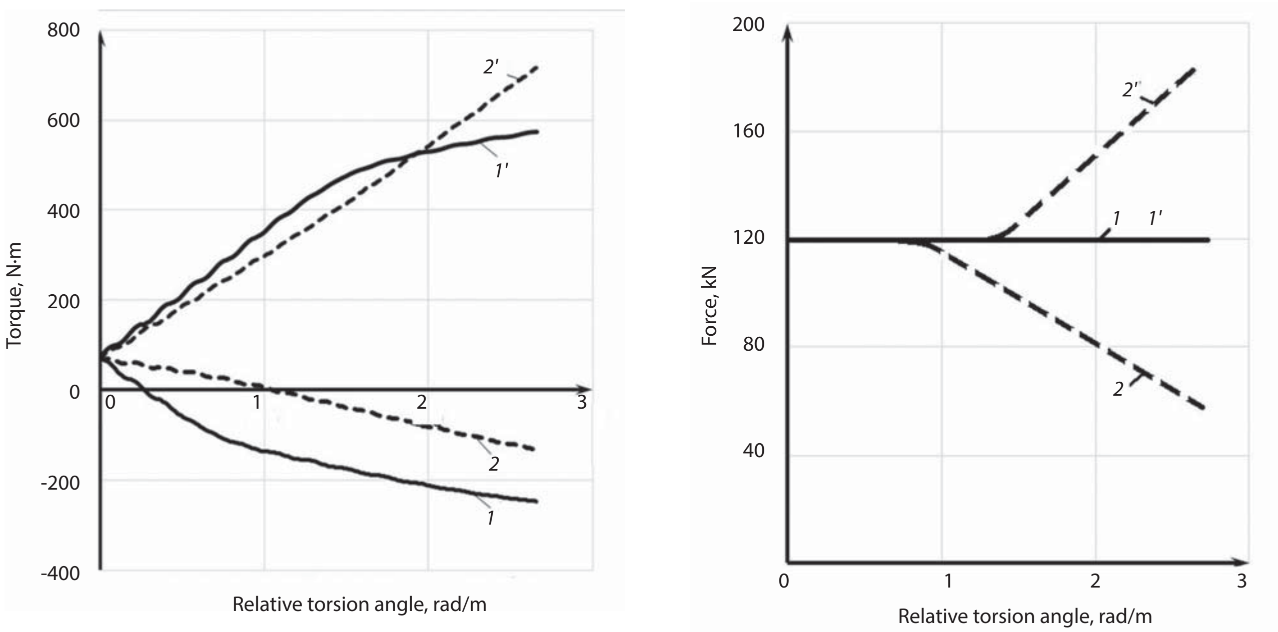

a b

Fig. 4. Variation of the torque (a) and axial force (b) in the rope for the conditions of joint extension and torsion: ——— – modeling; - - - - - analytical calculation; curves *1* and *2* - untwisting of the rope external layer; curves *1'* and *2'* - twisting of the rope external layer

- M = 68.4 N·m for $\theta = 0$;
- M = -252.4 N·m (during untwisting of the rope external layer) and M = -573.3 N·m (during twisting of the rope external layer) for $\theta = \pm 2{,}68$ rad/m (Fig. 4, *a*).

Taking into account the general tendency of increase of the external torque M with elevation of the relative torsion angle θ, the best rope anti-twisting parameters are observed during twisting of its external layer (curves *1* and *1'* on the Fig. 4, *a*). It is explained by difference between stiffness coefficients and laying directions of rope elements.

Use of the static equations (1) allows to determine analytically the values of axial forces P and torques M in a rope for the conditions of joint extension and torsion, applying the values of axial ε and angular θ motion of a movable stiff disc (which are coordinated by loading time) and the values of generalized coefficients A, B and C (curves *2* and *2'* on the Fig. 4), which were obtained earlier during simulation.

The static equations (1) are valid for the rope, which is characterized by deformations ε and θ equal for all rope elements. Comparative analysis of the curves on the Fig. 4, at the starting stages of loading, testifies mainly about similarity of variation features for the values of torques M and axial forces P for twisting the external layer to the relative angle θ = 1.5 rad/m (curves *1'* and *2'* on the Fig. 4), as well as axial forces P for untwisting the external layer to the relative angle θ = 0.6-0.8 rad/m (curves *1* and *2* on the Fig. 4, *b*), during modeling with the results of analytical calculation via the static equations. Differences between the variation curves of the force parameters in the case of exceeding the above-mentioned torsion angles θ is connected with the previously considered non-uniform mode of a contact load between the rope elements and exceeding of the yield strength values for wires material in some cases. The obtained results correspond with the experimentally confirmed results of computer-aided modeling for torsion of laid wire rope [9], where torque lowering with rising of torsion angle during the experiment is connected with non-elastic steel elongation.

Difference of the values of torque M during modeling and the results of analytical calculation for untwisting of the external layer (curves *1* and *2* on the Fig. 4, *a*) is explained by non-correspondence of the rope stiffness coefficients and calculated ones due to rope lamination [3]. Generalized stiffness coefficients for separated external layer of wires should be calculated in the same way as for screw springs (separated layer along the complete length is in free state and is not subjected to any contact load).

Conclusions

1. The results of computer-aided modeling of rope elements in the conditions of joint extension and torsion testify on non-uniformity of dimensions and intensity of distribution of torques and axial forces in rope elements, at preset constant sample torsion velocity. When rope is turning under the effect of external torque M, redistribution of internal forces P and torques M_t occurs with maximal intensity in the external and sub-surface layers. Decrease of the torque and axial force down to zero in the deposited external layer during its untwisting testifies on switching this layer off operation and possibility of rope lamination (in the case of absence of external pressure). At the same time, radial compression of the sub-surface layer from the side of the rope external layer during twisting decreases possibility of stability loss (lamination) of this layer.

2. Correspondence between variation mode of force parameters during modeling via FEM and the results of analytical calculation using linear static equations at the initial stage of joint extension and torsion was established in general case, for standard conditions. It was shown that when the extending force is constant, untwisting torque this to elongate the rope (ε increase), while twisting torque tries to compress it (ε decrease). Deviation of variation mode of external force and torque with enlargement of the torsion angle is explained by forming of contact stresses between rope layers, what rises wear possibility of rope elements. Evaluation of the contact stresses between the rope elements, which were obtained during modeling, were compared with the values of wire material yield strength; it allows during designing to predict saving of rope structural integrity and possibility of stability loss (lamination) of this layer.

REFERENCES

1. Danenko V. F., Gurevich L. M. On calculation of stress-strain state of steel closed ropes in extension and twisting. Part 1. Determination of generalized stiffness and deformation coefficients. *CIS Iron and Steel Review*. 2021. Vol. 22. pp. 20-25.
2. Kalentyev E. A., Tarasov V. V. Numerical analysis of the stress-strain state of a rope thread with linear touch during extension and twisting. *Vychislitelnaya mekhanika sploshnykh sred*. 2010. Vol. 3. No. 4. pp. 16-28.
3. Glushko M. F. Steel lifting ropes. Kiev. Tekhnika. 1966. 328 p.
4. Getman I. P., Ustinov Yu. A. About the methods of ropes calculation. *The problem of extension-twisting. Prikladnaya matematika i mekhanika*. 2008. Vol. 72. Iss. 1. pp. 81-90.
5. Khalfin M. N., Ivanov B. F., Kharkovskiy E. V. Determination of the strength reserve factor for a track rope with buckling account. *Izvestiya Tulskogo gosudarstvennogo universiteta. Tekhnichexkie nauki*. 2018. No. 1. pp. 122-126.
6. Polyakov S. V. Study of the lifting rope with appeared variations of geometrical parameters and mechanical properties of screw elements. *Nauchno-tekhnicheskiy vestnik Bryanskogo gosudarstvennogo universiteta*. 2019. No. 2. pp. 257-264.
7. Liu H., Wang H., Song B., Han X., Han B., Lin J. Modeling of braided wire ropes under tension and torsional loads. *The Journal of Strain Analysis for Engineering Design*. 2020. Vol. 56. No. 4. pp. 216-224. DOI: 10.1177/0309324720958257.
8. Danenko V. F., Gurevich L. M. Simulation of stress-strain state of closed rope during stretching and twisting. *Deformatsiya i razrushenie materialov*. 2021. No. 1. pp. 2-9.
9. Song B., Wang H., Cui W., Liu H., Yang T. Distributions of stress and deformation in a braided wire rope subjected to torsional loading. *The Journal of Strain Analysis for Engineering Design*. 2018. Vol. 54. No. 1. pp. 3-12. DOI: 10.1177/0309324718800814.
10. Wang H., Fu C., Cui W. et al. Numerical simulation and experimental study on stress deformation of braided wire rope. *The Journal of Strain Analysis for Engineering Design*. 2017. Vol. 52. No. 2. pp. 69–76.
11. Zhao X., Wang H. Research on expansion graph and mechanical modeling of anti-twist braided wire rope. *Journal of Mechanical Strength*. 2017. Vol. 39. No. 1. pp. 111–116 (in Chinese).
12. Ivanovskiy V. N., Sabirov A. A., Degovtsov A. V., Pekin S. S. Rope pump rod. Patent 2527275 RU. Bull. No. 24. Announced 24.06.2013. Published 27.08.2014.
13. Ivanovskiy V. N., Sabirov A. A., Degovtsov A. V. et al. Experience of well operation with side shaft with small diameter, sucker rod pumping unit with rope rod at Lukoil-Perm jsc. *Territoriya NEFTEGAZ*. 2015. No. 3. pp. 78-87.
14. Wang X., Wang D., Zhang D. et al. Effect of torsion angle on tension-torsion multiaxial fretting fatigue behaviors of steel wires. *International Journal of Fatigue*. 2018. Vol. 106. pp. 159–164.
15. Wang D., Song D., Wang X, et al. Tribo-fatigue behaviors of steel wires under coupled tension-torsion in different environmental media. *Wear*. 2019. Vol. 420. pp. 38–53.
16. Korotkiy A. A., Khalfin M. N., Ivanov B. F. et al. On torsion of load rope in pendulum cableways. *Bezopasnost tekhnogennykh i prirodnykh system*. 2019. No. 4. pp. 19-23.
17. Korotkiy A. A., Khalfin M. N., Ivanov B. F., Kharkovskiy E. V. Evaluation method for lifting ropes. *Izvestiya Tulskogo gosudarstvennogo universiteta. Tekhnicheskie nauki*. 2018. No. 6. pp. 428-434.
18. Vetrov A. P., Kanonenko L. F. Determination of causes of defects appearance in closed ropes. *Collection of works "Steel ropes"*. Iss. 8. Kiev. Tekhnika. 1971. pp. 54-59.
19. Danenko V. F., Gurevich L. M. Optimization of gaps in spiral ropes with closed construction for providing their structural integrity. *Metally*. 2021. No. 3. pp. 85-90.
20. Shtarkman E. M., Shkarupin B. E., Yakobson A. I. Analytical calculation of geometrical parameters of steel ropes taking into account gaps. *Collection of works "Steel ropes"*. Iss. 9. Kiev. Tekhnika. 1972. pp. 60-65.